Supplementary

Contents:

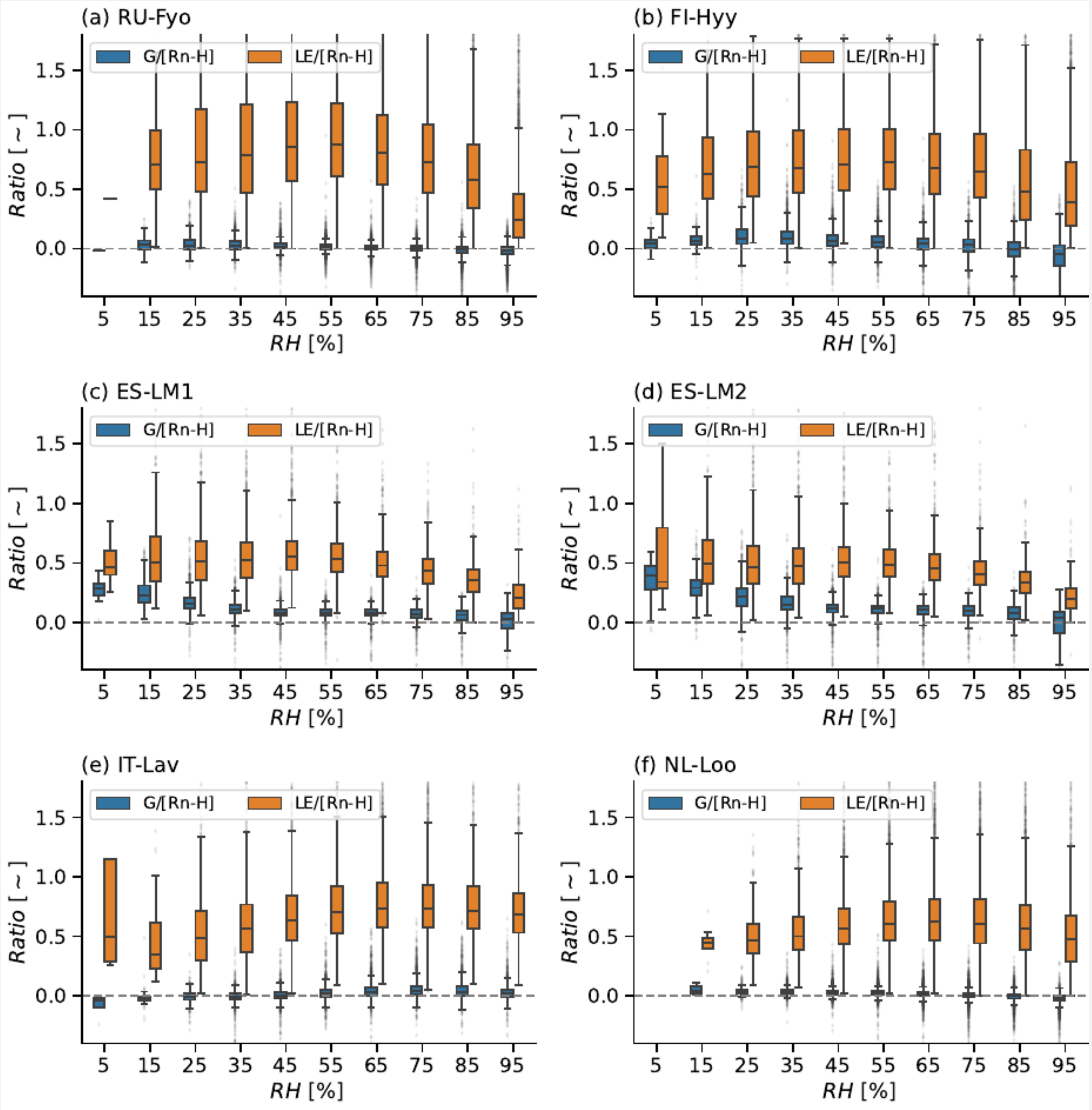

Figure S1 Comparison of the ratio of G to [Rn-H] and LE to [Rn-H] across RH bins at 6 sites.

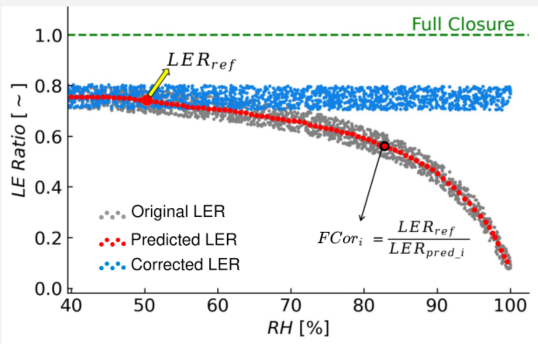

Figure S2 Schematic diagram indicating the calculation method for FCor.

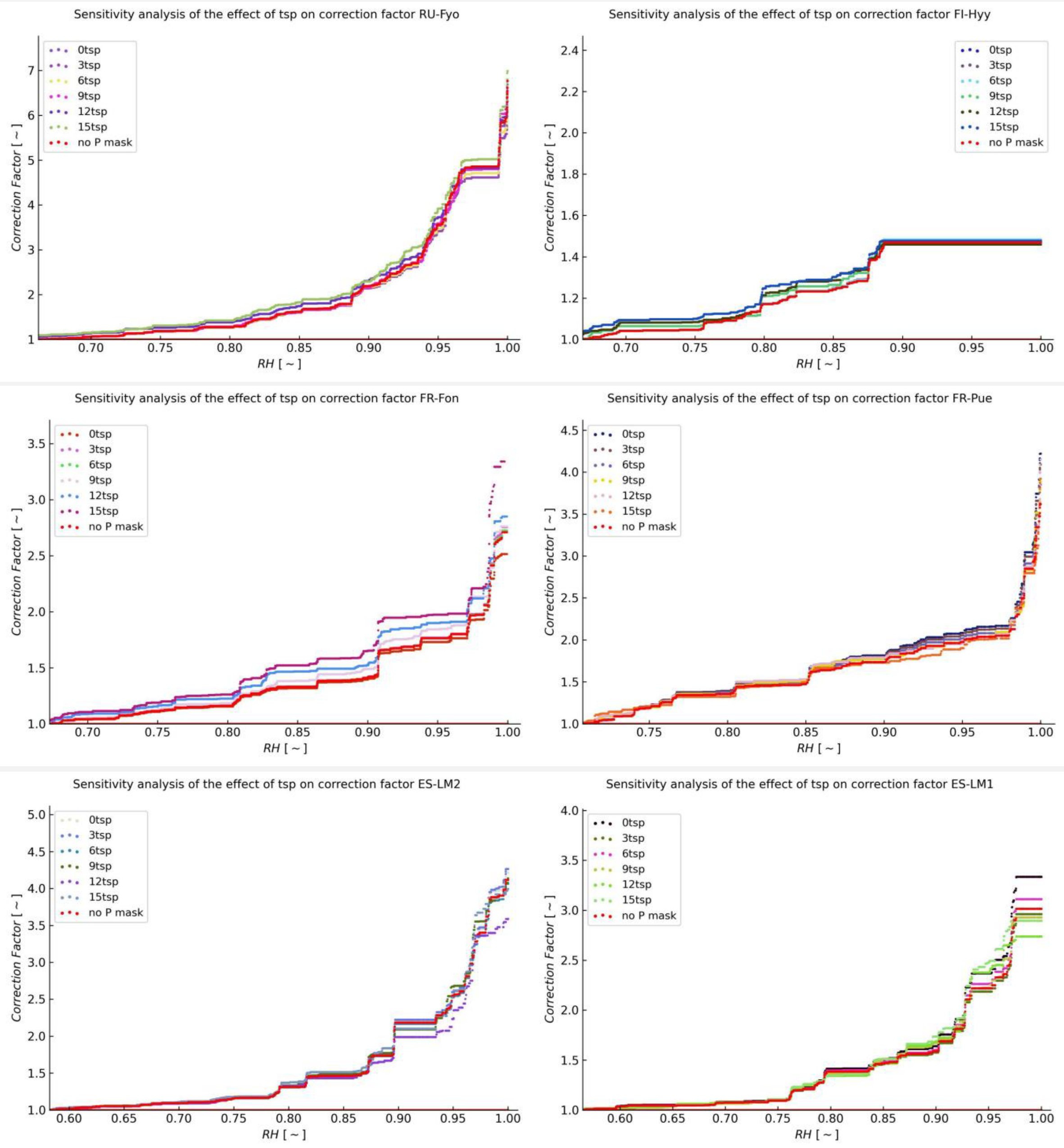

Figure S3 Sensitivity analysis of the precipitation impact on FCor. tsp: timesteps since one precipitation event, for instance, '12tsp' denotes that 12 timesteps after precipitation events were excluded. '0tsp' corresponds to the normal correction. The upper boundaries of FCor at different sites are different, thus the y-scale is not constant to obviously see the pattern at each site.

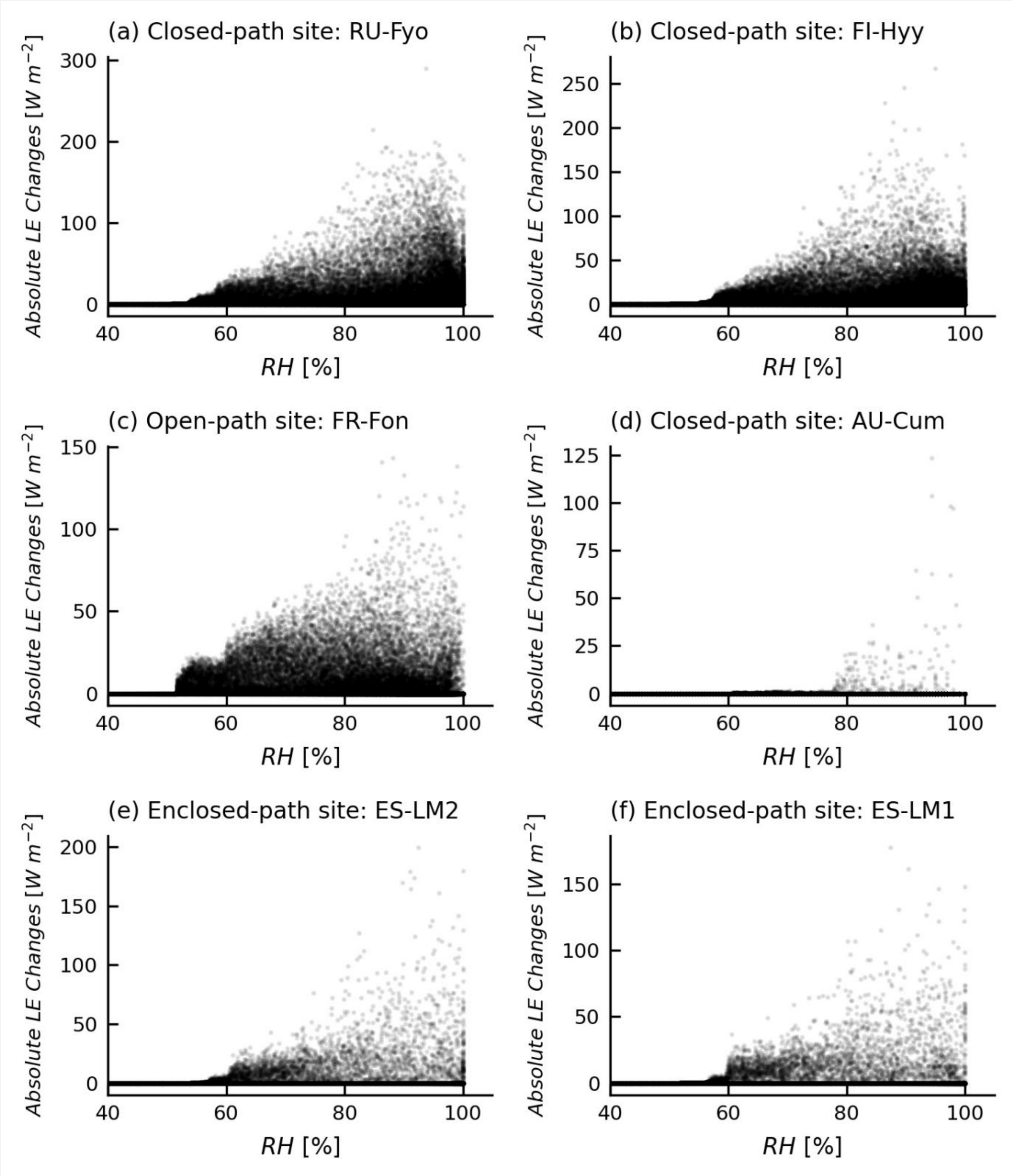

Figure S4 Distribution of absolute LE changes after correction along RH for (a, b) two closed-path sites, (c, d) two open-path sites, and (e,f) two enclosed-path sites. The upper boundaries of FCor at different sites are different, thus the y-scale is not constant to obviously see the pattern at each site.

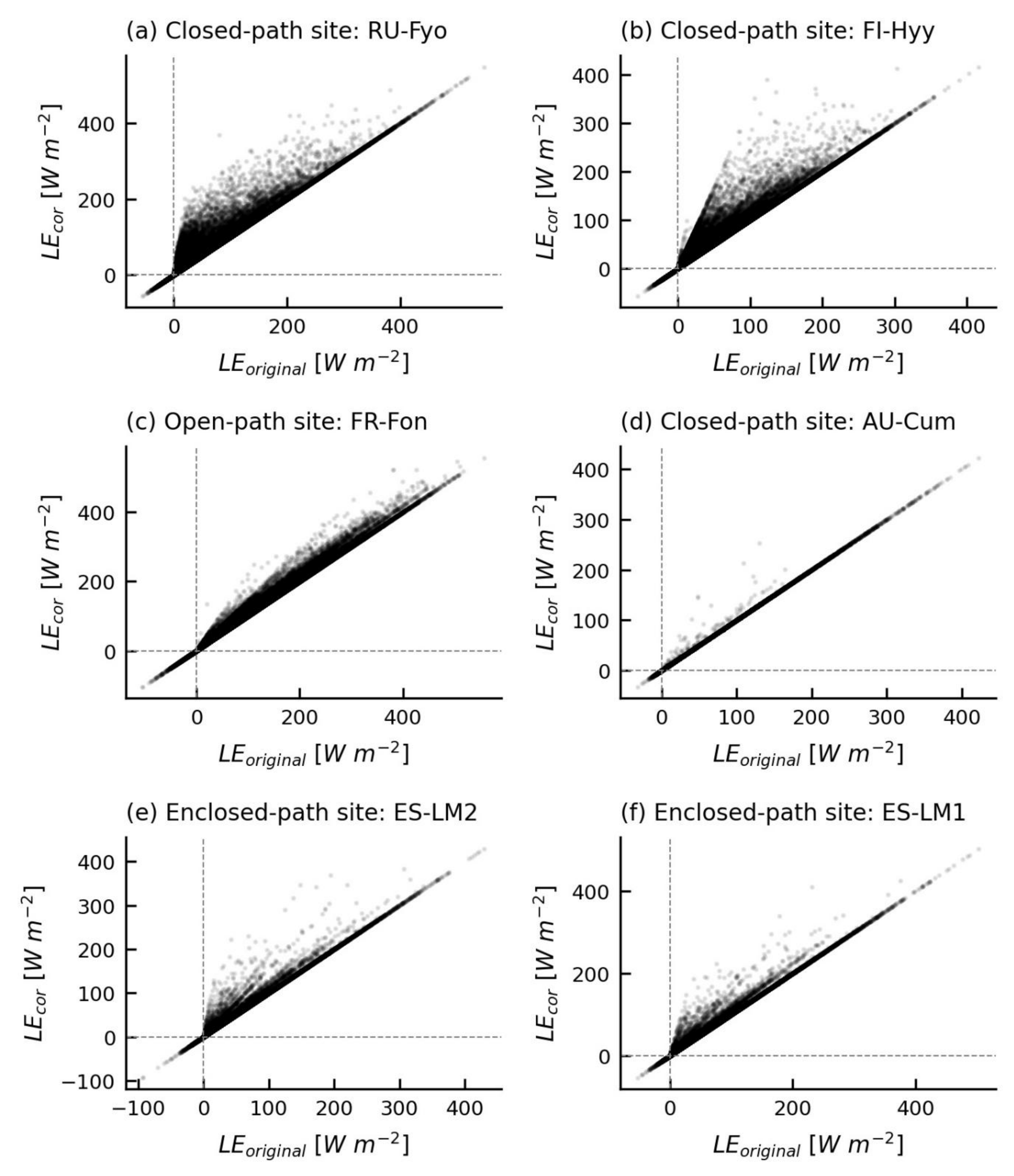

Figure S5 Comparison of observed and corrected LE for (a, b) two closed-path sites, (c, d) two open-path sites, and (e,f) two enclosed-path sites.

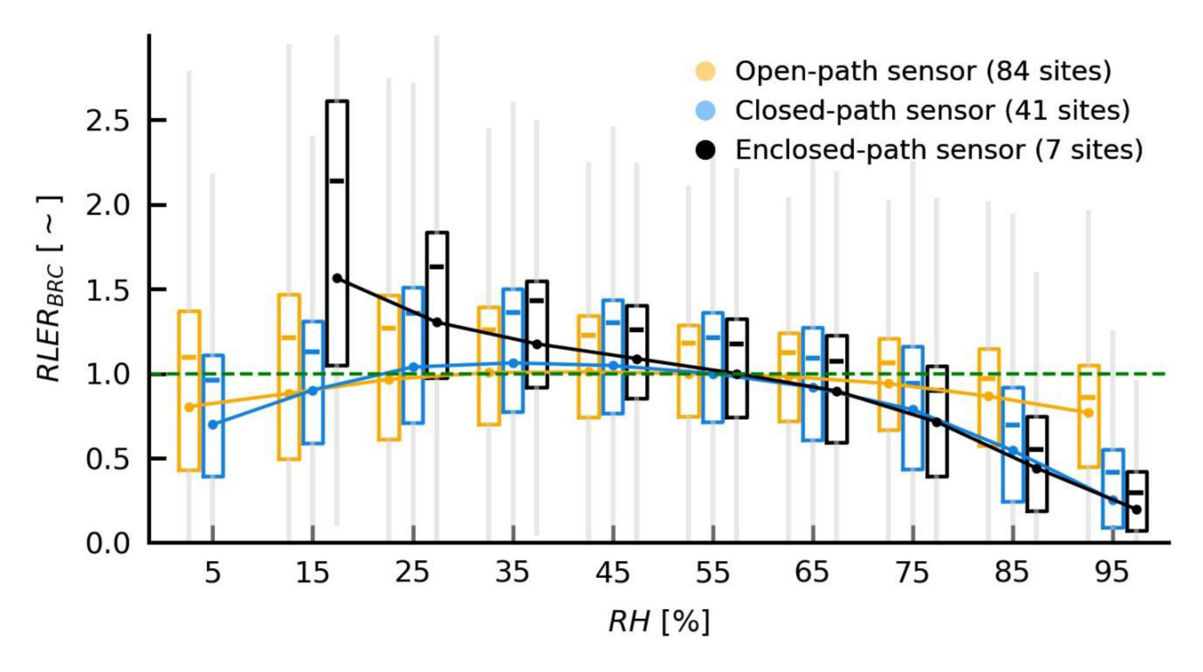

Figure S6 The BRC corrected relative LER (RLER) from all sites across RH bins at the hourly scale. The dots are the median value and the short horizontal lines are the mean value of the boxed data. The solid lines connect the median value to show that the overall pattern of RLER varies for open-, closed-, and enclosed-path sites. Boxes indicate interquartile ranges and gray vertical lines indicate the range of the data in each box. Data outside the interquartile range are not shown here to simplify the figure and clearly show the patterns. Bins with less than 500 hours of data are not plotted.

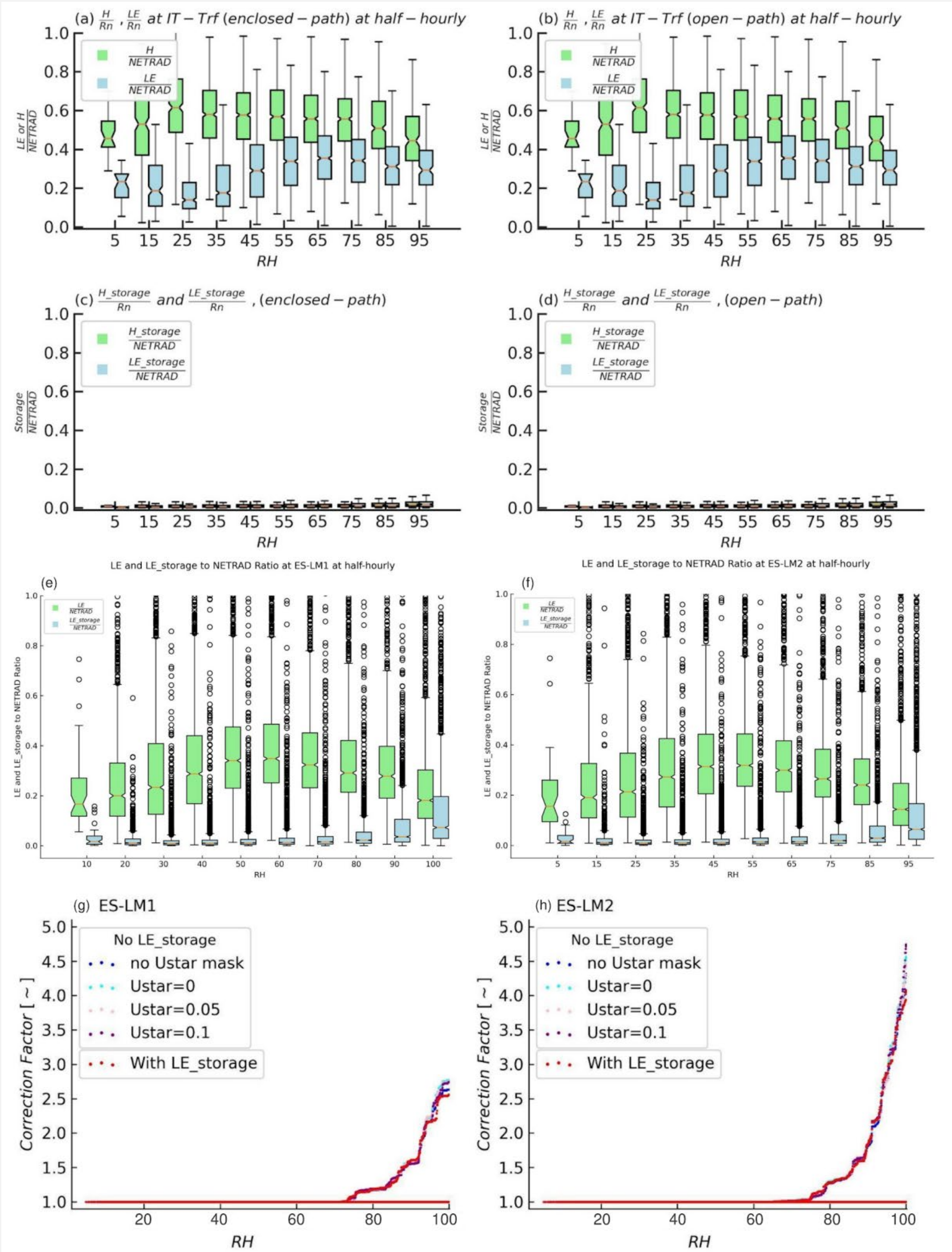

Figure S7 The ratio of (a, b) H and LE, (c, d) LE storage and H storage to Rn at half-hourly scale at IT-Trf with both enclosed-path and open-path gas analyzers. The ratio of LE and LE storage to Rn at half-hourly scale at (e) ES-LM1 and (f) ES-LM2 with both enclosed-path, as well as the effect of LE storage on the predicting of correction factors (g, h), respectively.

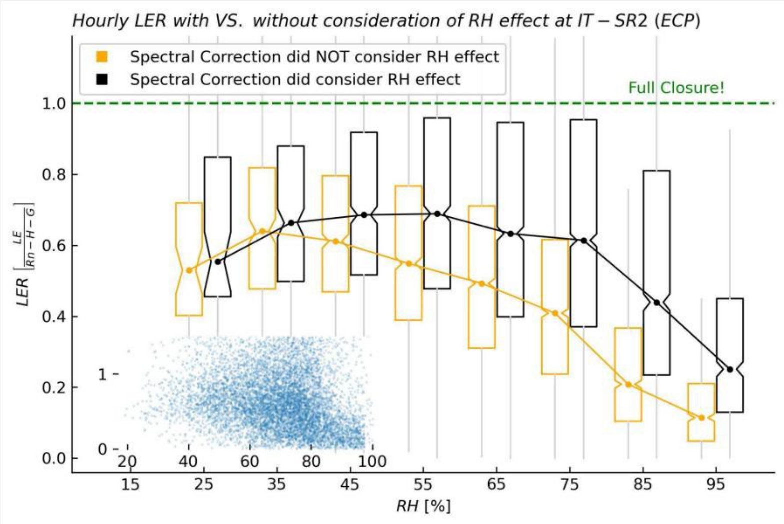

Figure S8 Comparison of the hourly LER with and without consideration of RH dependency in the spectral correction at the IT-SR2 site. Only hours without gap filling were considered, and for the box plot, only the number of hours in the RH bin more than 50 was considered. The lines connect the median values in each box. The sub-scatter plot shows the hourly LER among all RH conditions.

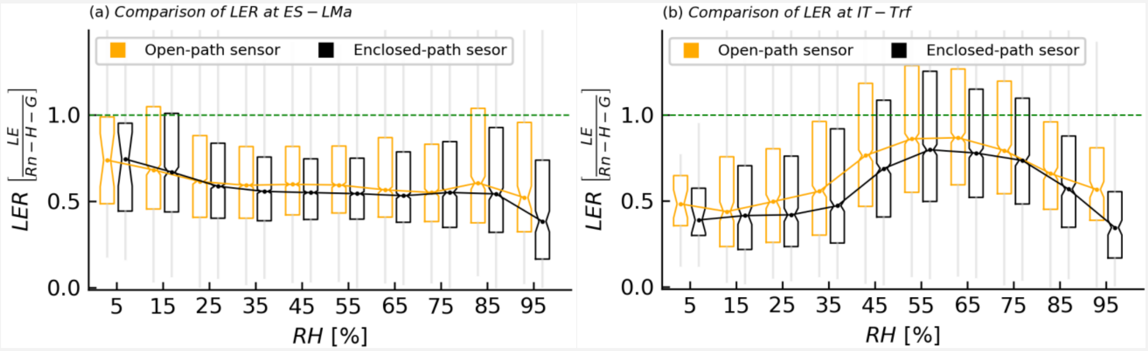

Figure S9 Original LER from (a) ES-LMa and (b) IT-Trf with both open- and enclosed-path gas analyzer installed across RH bins at the hourly scale. For each box, data are randomly sampled from 500 hours. The dots are the median value and the short horizontal lines are the mean value of the boxed data. The solid lines connect the median value to show that the overall pattern of LER varies. Boxes indicate quartile ranges and grey vertical lines indicate the ranges of the data in each box. Data outside the interquartile range are also not shown here to simplify the figure and clearly show the comparison.

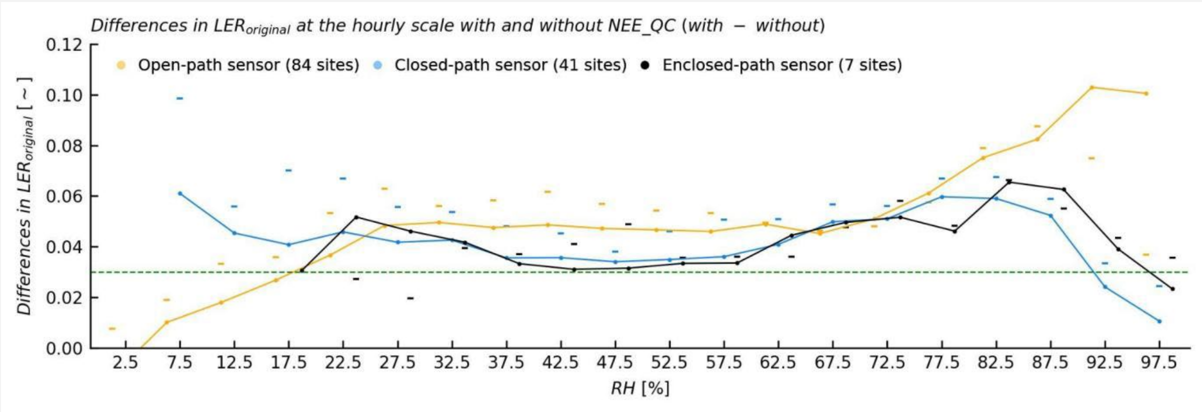

Figure S10 Differences in original LER at the hourly scale with and without NEE_QC mask. The dots denote the median values of the changes of original LER after removing 'low turbulence' hours at each box. The short line represents the mean values.

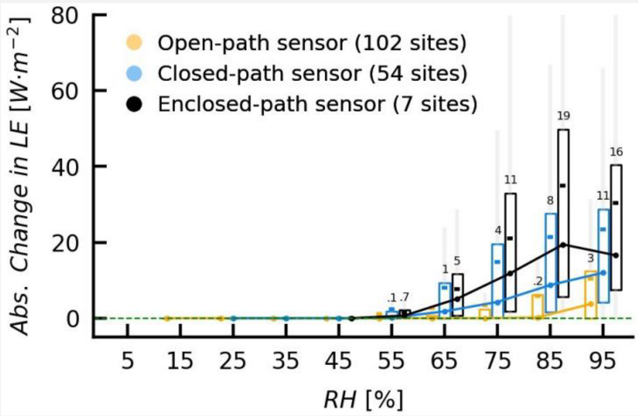

Figure S11 Absolute changes in LE after applying HRHC for all sites across RH bins at the hourly scale during rain events and during the following three hours. The dots are the median value and the short horizontal lines are the mean value of the boxed data. The solid lines connect the median value. The numbers above boxes represent median values. Boxes indicate interquartile ranges and grey vertical lines indicate the ranges of the data in each box. Data outside the interquartile range are not shown here to simplify the figure and clearly show the patterns. Bins with less than 500 hours of data are not plotted.

Table 1 Sites used in this work from Fluxnet2015 and from ICOS-drougt2018 consists of open-path sites, closed-path sites, and en-closed-path sites. The sensor type represents the gas measurement system installed in each site. G observation denoted as the G obs. indicates that if there are G measurements in each site. The years of LE show the onset and end of the year of LE measurements. The Plant Functional Type (PFT) classified according to IGBP global vegetation classification scheme is gathered from the site information published on the FLUXNET2015

Open-path sites:

Num.	Site	Sensor Type	G obs.	Years of LE	If Confir med	Including RH on the spectral transfer function	PFT
1	AR-SLu	LI-7500	Yes	2009 - 2011			MF
2	AU-ASM	LI-7500	Yes	2010 - 2014	1	No	ENF
3	AU-Cpr	LI-7500	Yes	2010 - 2014	1		SAV
4	AU-Cum	LI-7500	Yes	2012 - 2014	1		EBF
5	AU-DaP	LI-7500	Yes	2007 - 2013	1		GRA
6	AU-DaS	LI-7500	Yes	2008 - 2011	1		SAV
7	AU-Dry	LI-7500	Yes	2008 - 2014	1		SAV
8	AU-Emr	LI-7500	Yes	2011 - 2013	1		GRA
9	AU-Gin	LI-7500	Yes	2011 - 2013	1		WSA
10	AU-RDF	LI-7500	Yes	2011 - 2013			WSA
11	AU-Rob	LI-7500	Yes	2014 - 2014	1	No	EBF
12	AU-TTE	LI-7500	Yes	2012 - 2014	1	No	OSH
13	AU-Tum	LI-7500	Yes	2001 - 2014	1		EBF
14	AU-Wac	LI-7500	Yes	2005 - 2008	1		EBF
15	AU-Wom	LI-7500	Yes	2010 - 2014	1	No	EBF
16	AU-Ync	LI-7500	Yes	2012 - 2014	1		GRA
17	CA-SF1	LI-7500	Yes	2003 - 2006			ENF
18	CA-SF2	LI-7500	Yes	2001 - 2005			ENF
19	CA-SF3	LI-7500	Yes	2002 - 2006			OSH
20	CG-Tch	LI-7500	No	2006 - 2009			SAV
21	CH-Cha	LI-7500	Yes	2005 - 2018	1	No	GRA
22	CH-Dav	LI-7500	Yes	2006 - 2018	1	No	ENF
23	CH-Fru	LI-7500	Yes	2005 - 2018	1	No	GRA
24	CH-Oe1	LI-7500	No	2002 - 2008	1	No	GRA

25	CN-Cha	LI-7500	No	2003 - 2005			MF
26	CN-Cng	LI-7500	Yes	2007 - 2010			GRA
27	CN-Dan	LI-7500	No	2004 - 2005			GRA
28	CN-Din	LI-7500	No	2003 - 2005			EBF
29	CN-Du2	LI-7500	Yes	2006 - 2008			GRA
30	CN-HaM	LI-7500	Yes	2002 -2004	1	No	GRA
31	CN-Qia	LI-7500	No	2003 - 2005			ENF
32	CN-Sw2	LI-7500	No	2010 - 2012	1		GRA
33	DE-Lkb	LI-7500	Yes	2009 - 2013	1	No	ENF
34	DE-RuR	LI-7500	Yes	2011 - 2018	1	No	GRA
35	DE-RuS	LI-7500	Yes	2011 - 2018	1	No	CRO
36	DE-Seh	LI-7500	Yes	2007 - 2010	1	No	CRO
37	DE-SfN	LI-7500	Yes	2012 - 2014			WET
38	ES-Amo	LI-7500	Yes	2007 - 2012	1		OSH
39	ES-LJu	LI-7500	Yes	2004 - 2013	1		OSH
40	ES-LgS	LI-7500	Yes	2007 - 2009	1		OSH
41	FR-Fon	LI-7500	No	2005 - 2014			DBF
42	FR-Gri	LI-7500	Yes	2004 - 2014	1		CRO
43	GF-Guy	LI-7500	No	2004 - 2014	1		EBF
44	IT-BCi	LI-7500	Yes	2004 - 2015	1	No	CRO
45	IT-CA1	LI-7500	Yes	2011 - 2014	1	No	DBF
46	IT-CA2	LI-7500	Yes	2011 - 2014	1	No	CRO
47	IT-CA3	LI-7500	Yes	2011 - 2014	1	No	DBF
48	IT-La2	LI-7500	No	2000 - 2002			ENF
49	IT-Lav	LI-7500	Yes	2003 - 2014			ENF
50	IT-MBo	LI-7500	Yes	2003 - 2013	1		GRA
51	IT-Noe	LI-7500	Yes	2004 - 2014			CSH
52	IT-Ren	LI-7500	Yes	2002 - 2013	1	No	ENF
53	IT-Tor	LI-7500	Yes	2008 - 2018	1		GRA
54	MY-PSO	LI-7500	Yes	2003 - 2009			EBF
55	NL-Hor	LI-7500	Yes	2004 - 2011			GRA
56	NL-Loo	LI-7500	Yes	2001 - 2018			ENF

57	PA-SPn	LI-7500	No	2007 - 2009	1	No	DBF
58	PA-SPs	LI-7500	No	2007 - 2009	1	No	GRA
59	RU-Cok	LI-7500	Yes	2003 - 2014			OSH
60	RU-Ha1	LI-7500	Yes	2002 - 2004	1	No	GRA
61	SD-Dem	LI-7500	Yes	2005 - 2009	1	No	SAV
62	US-AR1	LI-7500	Yes	2009 - 2012	1	Moore (1986)	GRA
63	US-AR2	LI-7500	Yes	2009 - 2012	1	Moore (1986)	GRA
64	US-ARM	LI-7500	Yes	2003 - 2012	1	Moore (1986)	CRO
65	US-ARb	LI-7500	Yes	2005 - 2006	1	Moore (1986)	GRA
66	US-ARc	LI-7500	Yes	2005 - 2006	1		GRA
67	US-Atq	LI-7500	Yes	2003 - 2008	1		WET
68	US-CRT	LI-7500	Yes	2011 - 2013	1		CRO
69	US-GLE	LI-7500	Yes	2004 - 2014	1	No	ENF
70	US-Goo	Other	Yes	2002 - 2006			GRA
71	US-IB2	LI-7500	Yes	2004 - 2011			GRA
72	US-Ivo	LI-7500	Yes	2004 - 2007	1		WET
73	US-LWW	Other	Yes	1997 - 1998			GRA
74	US-Me1	LI-7500	Yes	2004 - 2005	1	No	ENF
75	US-Me2	LI-7500	Yes	2002 - 2014	1	No	ENF
76	US-Me3	LI-7500	No	2004 - 2009	1	No	ENF
77	US-Me4	LI-7500	Yes	2000 - 2000	1	No	ENF
78	US-Me5	LI-7500	Yes	2000 - 2002	1	No	ENF
79	US-Me6	LI-7500	Yes	2010 - 2014	1	No	ENF
80	US-Myb	LI-7500	No	2010 - 2014	1		WET
81	US-Ne1	LI-7500	Yes	2001 - 2013	1	No	CRO
82	US-Ne2	LI-7500	Yes	2001 - 2013	1	No	CRO
83	US-Ne3	LI-7500	Yes	2001 - 2013	1	No	CRO
84	US-Oho	LI-7500	Yes	2004 - 2013	1		DBF
85	US-SRC	LI-7500	Yes	2008 - 2014	1		OSH
86	US-SRG	LI-7500	Yes	2008 - 2014	1	No	GRA
87	US-SRM	LI-7500	Yes	2004 - 2014	1	No	WSA
88	US-Ton	LI-7500	Yes	2001 - 2014	1		WSA

89	US-Tw4	LI-7500	Yes	2013 - 2014	1		WET
90	US-Twt	LI-7500	Yes	2009 - 2014	1		CRO
91	US-Var	LI-7500	Yes	2000 - 2014	1		GRA
92	US-Whs	LI-7500	Yes	2007 - 2014	1	No	OSH
93	US-Wi0	LI-7500	Yes	2002 - 2002	1		ENF
94	US-Wi3	LI-7500	Yes	2002 - 2004	1		DBF
95	US-Wi4	LI-7500	Yes	2002 - 2005	1		ENF
96	US-Wi5	LI-7500	No	2004 - 2004	1		ENF
97	US-Wi6	LI-7500	Yes	2002 - 2003	1		OSH
98	US-Wi7	LI-7500	No	2005 - 2005	1		OSH
99	US-Wi8	LI-7500	Yes	2002 - 2002	1		DBF
100	US-Wi9	LI-7500	No	2004 - 2005	1		ENF
101	US-Wkg	LI-7500	Yes	2004 - 2014	1		GRA
102	US-WPT	LI-7500	No	2011 - 2013	1		WET

Note:
Li-7500 indicates the three different models (Li-7500 RS, Li-7500 A, Li-7500) as the water flux measured by the three models are quite consistent (Kutikoff et al. 2020).
If Confirmed indicates whether the information we collected was confirmed by PIs.

Closed-path sites:

Num.	Site	Sensor Type	G obs.	Years of LE	If Confirmed	Including RH on the spectral transfer function	PFT
1	AT-Neu	LI-6262	Yes	2002 - 2012	1	No	GRA
2	BE-Bra	LI-6262	Yes	1996 - 2018			MF
3	BE-Lon	LI-7000	Yes	2004 - 2013	1		CRO
4	BE-Vie	LI-6262	Yes	1996 - 2013	1		MF
5	BR-Sa3	LI-7000	Yes	2000 - 2004			EBF
6	CA-NS2	LI-7000	No	2001 - 2005			ENF
7	CA-NS3	LI-7000	No	2001 - 2005			ENF
8	CA-NS4	LI-7000	No	2002 - 2005			ENF
9	CA-NS5	LI-7000	No	2001 - 2005			ENF
10	CA-NS6	LI-7000	No	2001 - 2005			OSH
11	CA-NS7	LI-7000	No	2002 - 2005			OSH
12	CA-Oas	LI-6262	No	1996 - 2010			DBF
13	CA-Obs	LI-6262	Yes	1999 - 2010			ENF
14	CA-Qfo	LI-7000	Yes	2003 - 2010			ENF
15	CA-TP1	LI-7000	Yes	2008 - 2014	1	No	ENF
16	CA-TP3	LI-7000	Yes	2008 - 2014	1	No	ENF
17	CA-TP4	LI-7000	Yes	2002 - 2014	1	No	ENF
18	DE-Geb	LI-7000	Yes	2002 - 2015	1	Ibrom et al. (2007)	CRO
19	DE-Gri	LI-7000	Yes	2005 - 2018	1	Fratini et al. (2012)	GRA
20	DE-Hai	LI-6262	Yes	2000 - 2018	1	Ibrom et al. (2007)	DBF
21	DE-Kli	LI-7000	Yes	2004 - 2018	1	Fratini et al. (2012)	CRO
22	DE-Lnf	LI-6262	Yes	2002 - 2012	1	Ibrom et al. (2007)	DBF
23	DE-Obe	LI-7000	Yes	2008 - 2018	1	Fratini et al. (2012)	ENF
24	DE-Tha	LI-6262	Yes	1996 - 2018	1	Fratini et al. (2012)	ENF
25	DK-Sor	LI-6262	Yes	1996 - 2018	1	Ibrom et al. (2007)	DBF
26	FI-Hyy	LI-6262	Yes	1996 - 2018	1	Mammarella et al (2009)	ENF
27	FI-Let	LI-7000	Yes	2009 - 2018	1	No	ENF
28	FI-Lom	LI-7000	Yes	2007 - 2009	1		WET
29	FI-Sod	LI-7000	Yes	2001 - 2014	1		ENF
30	FR-LBr	LI-6262	Yes	1996 - 2002			ENF

31	FR-Pue	LI-6262	Yes	2000 - 2014	1	No	EBF
32	GH-Ank	LI-6262	Yes	2011 - 2014	1		EBF
33	GL-NuF	LI-7000	No	2008 - 2014			WET
34	GL-ZaF	LI-6262	Yes	2008 - 2011			WET
35	GL-ZaH	LI-6262	No	2000 - 2014			GRA
36	IT-Col	LI-6262	Yes	1996 - 2014	1	Yes	DBF
37	IT-Cpz	LI-6262	Yes	1997 - 2008	1	Yes	EBF
38	IT-PT1	LI-6262	Yes	2002 - 2004	1	No, Moncrieff et al (1997)	DBF
39	IT-Ro1	LI-6262	No	2000 - 2008	1	Yes	DBF
40	IT-Ro2	LI-6262	Yes	2002 - 2012	1	Yes	DBF
41	IT-SRo	LI-6262	Yes	1999 - 2007	1	No, Moncrieff et al (1997)	ENF
42	RU-Che	LI-6262	Yes	2002 - 2004			WET
43	RU-Fyo	LI-6262	Yes	1998 - 2018	1	No, Moncrieff et al (1997)	ENF
44	US-Blo	LI-6262	Yes	1997 - 2007	1	No	ENF
45	US-Ha1	LI-6262	No	1992 - 2012			DBF
46	US-KS1	LI-6262	Yes	2002 - 2002			ENF
47	US-Lin	LI-6262	Yes	2009 - 2010	1	No	CRO
48	US-Los	LI-6262	Yes	2000 - 2014	1	No	WET
49	US-MMS	LI-6262	Yes	1999 - 2014	1	No	DBF
50	US-NR1	LI-6262	Yes	1998 - 2014			ENF
51	US-Syv	LI-6262	Yes	2001 - 2012	1	No	MF
52	US-UMB	LI-6252	No	2000 - 2014	1	No	DBF
53	US-WCr	LI-6262	Yes	1999 - 2014	1	No	DBF
54	ZM-Mon	LI-7000	Yes	2000 - 2009			WSA

Enclosed-path sites:

Num.	Site	Sensor Type	G obs.	years of LE	If Confirmed	Including RH on the spectral transfer function	PFT
1	CA-TPD	LI-7200	Yes	2012-2014	1	No	DBF
2	CZ-wet	LI-7200	Yes	2011-2018	1	Ibrom et al. (2007)	WET
3	ES-LM1	LI-7200	Yes	2014-2018	1	Yes	SAV
4	ES-LM2	LI-7200	Yes	2014-2018	1	Yes	SAV

5	IT-Cp2	LI-7200	Yes	2012-2018	1	No	EBF
6	IT-SR2	LI-7200	Yes	2013-2018	1	No	ENF
7	US-Prr	LI-7200	Yes	2010-2014	1	No, Moncrieff et al (1997)	ENF

Table 2 Description of variables.

Variable	Units	Long Name	Gap Filling
Rn	W m-2	Net radiation	Using ERA downscaling
H	W m-2	Sensible heat flux	Using MDS method
LE	W m-2	Latent heat flux	
G	W m-2	Soil heat flux	
LE_storage	W m-2	Latent heat storage flux	
H_storage	W m-2	Sensible heat storage flux	
SW_IN	W m-2	Shortwave radiation, incoming	Using MDS method
SW_IN_POT	W m-2	Shortwave radiation - incoming - potential (top of atmosphere)	Using ERA downscaling
USTAR	m s-1	Friction velocity	
WS	m s-1	Wind speed	Using ERA downscaling
PA	kPa	Atmospheric pressure	Using ERA downscaling
RH	%	Relative humidity	
TA	deg C	Air temperature	Using MDS method and ERA downscaling
VPD	hPa	Vapor Pressure Deficit	Using MDS method and ERA downscaling
P	mm	Precipitation	
GPP	μmolCO2 m-2 s-1	Gross Primary Productivity	
ET	mm	Evapotranspiration	
NETRAD_QC	Adimensional	Quality flag for NETRAD	
H_QC	Adimensional	Quality flag for H	
LE_QC	Adimensional	Quality flag for LE	
NEE_QC	Adimensional	Quality flag for NEE	

Table 3 Description of sites with both EC and sap flow data:

Closed-path sites

Num.	Site code	Site (EC)	years of sap flow
1	CAN_TUR_P74	CA-TP3	2012-2014
2	CAN_TUR_P39_POS	CA-TP4	
3	FIN_HYY_SME	FI-Hyy	
4	FRA_PUE	FR-Pue	2014-2018
5	RUS_FYO	RU-Fyo	2014-2018
6	USA_SYL_HL1	US-Syv	2010 - 2014

Open-path sites

Num.	Site code	Site (EC)	years of sap flow
1	AUS_RIC_EUC_ELE	AU-Cum	2012.10–2014.08
2	CHE_DAV_SEE	CH-Dav	2010.01–2010.12
3	ITA_TOR	IT-Tor	2014
4	NLD_LOO	NL-Loo	2010 - 2014

Reference

Moore, C.J, 1986. Frequency response corrections for eddy correlation systems. Boundary-Layer Meteorol 37, 17–35. https://doi.org/10.1007/BF00122754

Kutikoff, S., Lin, X., Evett, S.R., Gowda, P., Brauer, D., Moorhead, J., Marek, G., Colaizzi, P., Aiken, R., Xu, L., Owensby, C., 2021. Water vapor density and turbulent fluxes from three generations of infrared gas analyzers. Atmospheric Measurement Techniques 14, 1253–1266. https://doi.org/10.5194/amt-14-1253-2021

Ibrom, A., Dellwik, E., Flyvbjerg, H., Jensen, N.O., Pilegaard, K., 2007. Strong low-pass filtering effects on water vapour flux measurements with closed-path eddy correlation systems. Agricultural and Forest Meteorology 17. https://doi.org/10.1016/j.agrformet.2007.07.007

Fratini, G., Ibrom, A., Arriga, N., Burba, G., Papale, D., 2012. Relative humidity effects on water vapour fluxes measured with closed-path eddy-covariance systems with short sampling lines. Agricultural and Forest Meteorology 165, 53–63. https://doi.org/10.1016/j.agrformet.2012.05.018

Mammarella, I., Launiainen, S., Gronholm, T., Keronen, P., Pumpanen, J., Rannik, U.L., Vesala, T., 2009. Relative Humidity Effect on the High-Frequency Attenuation of Water Vapor Flux Measured by a Closed-Path Eddy Covariance System. Journal of Atmospheric and Oceanic Technology 26. https://doi.org/10.1175/2009JTECHA1179.1